



Published in final edited form as:

Free Radic Biol Med. 2008 October 15; 45(8): 1167–1177. doi:10.1016/j.freeradbiomed.2008.07.018.

DNA Damage-induced Reactive Oxygen Species (ROS) Stress Response in *Saccharomyces cerevisiae*

Lori A. Rowe^{1,2}, Natalya Degtyareva^{1,3}, and Paul W. Doetsch^{1,3,4,5}

¹Department of Biochemistry, Emory University School of Medicine, Atlanta, GA

²Graduate Program in Biochemistry, Cell and Developmental Biology, Emory University School of Medicine, Atlanta, GA

³Emory Winship Cancer Institute, Emory University School of Medicine, Atlanta, GA

⁴Department of Radiation Oncology, Emory University School of Medicine, Atlanta, GA

⁵Department of Hematology and Medical Oncology, Emory University School of Medicine, Atlanta, GA

Abstract

Cells are exposed to both endogenous and exogenous sources of reactive oxygen species (ROS). At high levels, ROS can lead to impaired physiological function through cellular damage of DNA, proteins, lipids, and other macromolecules, which can lead to certain human pathologies including cancers, neurodegenerative disorders, and cardiovascular disease, as well as aging. We have employed *Saccharomyces cerevisiae* as a model system to examine the levels and types of ROS that are produced in response to DNA damage in isogenic strains with different DNA repair capacities. We find that when DNA damage is introduced into cells from exogenous or endogenous sources there is an increase in the amount of intracellular ROS which is not directly related to cell death. We have examined the spectrum of ROS in order to elucidate its role in the cellular response to DNA damage. As an independent verification of the DNA damage-induced ROS response, we show that a major activator of the oxidative stress response, Yap1, relocalizes to the nucleus following exposure to the DNA alkylating agent methyl methanesulfonate. Our results indicate that the DNA damage-induced increase in intracellular ROS levels is a generalized stress response that is likely to function in various signaling pathways.

Keywords

reactive oxygen species; DNA damage; genotoxic stress; DNA repair; oxidative stress response; Yap1 transcription factor

Introduction

Cells are continuously exposed to numerous exogenous and endogenous agents that damage DNA. DNA damage alters replication and transcription, causes cell death and can lead to mutations and neoplastic transformation in many organisms. Reactive oxygen species (ROS)-

Address correspondence to: Dr. Paul Doetsch, 1510 Clifton Rd, Atlanta, GA 30322. Phone: 404-727-0409; Fax: 404-727-2618; e-mail: medpwd@emory.edu.

Publisher's Disclaimer: This is a PDF file of an unedited manuscript that has been accepted for publication. As a service to our customers we are providing this early version of the manuscript. The manuscript will undergo copyediting, typesetting, and review of the resulting proof before it is published in its final citable form. Please note that during the production process errors may be discovered which could affect the content, and all legal disclaimers that apply to the journal pertain.

mediated deleterious effects are thought to contribute to human degenerative conditions including neurological disorders [1], cardiac dysfunction [2], and cancer [3], as well as the process of aging [4]. While ROS have been shown to be deleterious to cells, they also can function as stress-induced signaling molecules [5–8]. Recent reports indicate that DNA damage alone results in increased levels of intracellular ROS [9,10]. In response to oxidative stress, cells activate both the DNA repair processes and transcription factors. These factors in turn, modulate levels of expression of ROS-scavenging and processing enzymes [11,12]. For example, increased levels of intracellular ROS cause post-translational modifications of one such transcription factor, Yap1, resulting in induction of numerous genes [13–17].

In order to maintain genomic stability under ROS-induced stress, cells have evolved a number of pathways to repair or respond to the presence of DNA damage. In *Saccharomyces cerevisiae*, these pathways include direct reversal, base excision repair (BER), nucleotide excision repair (NER), mismatch repair (MMR), translesion synthesis (TLS), and recombination (REC) [18]. While some of these pathways mediate the repair of the damaged DNA (direct reversal, BER, NER, and MMR) others function to bypass the damage such that the DNA lesion is tolerated and replication can occur (TLS and REC). All of these pathways are individually important to the cell; however there is overlap in the types of DNA damage handled by each pathway [9,18]. BER is primarily responsible for the repair of small, non-bulky base lesions and abasic sites, such as those caused by oxidizing and alkylating agents [19]. NER is primarily responsible for the repair of bulky, DNA helix distorting lesions such as UV light-induced cyclobutane pyrimidine dimers (CPDs) and 6-4 photoproducts (6-4 PPs) [19].

We have previously reported that various types of spontaneous and chemically induced DNA damage cause increases in intracellular ROS in repair-proficient (wild type, WT) and repair-deficient *S. cerevisiae* strains [9,10]. Cells deficient in both BER and NER (BER-/NER-) spontaneously accumulate approximately 800-fold more oxidative DNA damage than WT cells that correlated with a substantial increase in intracellular ROS in repair-deficient cells [9]. In a separate study, Salmon *et al.* examined the levels of ROS in WT and repair deficient yeast strains (BER-, BER-/REC-, and NER-/REC- deficient strains) following exposure to the oxidative DNA damaging agent hydrogen peroxide (H₂O₂) or the DNA alkylating agent methyl methanesulfonate (MMS) [10]. These studies revealed a dose-dependent increase in intracellular levels of ROS in all four isogenic strains after exposure to either H₂O₂ or MMS, suggesting that DNA damage alone is capable of causing an increase in intracellular ROS.

A major issue emerging from the above observations is whether the increase in ROS is a response to specific types of DNA modifications or a general DNA damage-induced stress response. Another important issue concerns the nature of the subspecies of ROS, such as superoxide (O₂^{•-}), H₂O₂, and hydroxyl radical (•OH), produced in response to DNA damage. A major goal of this study was to further define the nature of DNA damage capable of inducing ROS and to characterize the subspecies of ROS that were produced in response to such damage. Such information is crucial for delineation of the biological role of ROS and the mechanisms leading to their production in a putative DNA damage-induced ROS stress response.

As an independent method for verifying the production of DNA damage-induced intracellular ROS, we also examined the cellular response of a ROS sensor and transcription factor, Yap1. Yap1 is important in the oxidative stress response in *S. cerevisiae* [11,16,17]. Oxidative stress within a cell can be viewed as an imbalance between ROS production and ROS scavenging/metabolizing capacity. When an imbalance leading to oxidative stress occurs, Yap1 is activated to rapidly up regulate gene expression of enzymes (e.g. catalase, superoxide dismutase, and glutathione peroxidase) and small molecules (e.g. glutathione and thioredoxins) capable of scavenging ROS [20]. H₂O₂ activates Yap1 by inducing disulfide bond formation between

C303 and C598, causing the release of the nuclear export protein Crm1p and resulting in nuclear accumulation of Yap1 [14,21]. Once in the nucleus, Yap1 functions as a transcription factor activating numerous genes that are involved in the oxidative stress response [16,17,22,23]. Thus, Yap1 serves as a biological sensor for elevated ROS and also as a key mediator of the ROS-activated signaling pathway.

In this study, we have defined the levels and types of ROS induced by DNA damage that are influenced by two major DNA excision repair pathways (BER and NER) and find that there is a dose-dependent increase in ROS in all cell types following exposure to the DNA alkylating agent MMS or short wavelength ultraviolet light (UV-C). We also find that there is a dose-dependent increase in several types of ROS ($O_2^{\cdot-}$, H_2O_2 , and $\cdot OH$) that were evaluated. However, the specific patterns and magnitudes of the observed ROS increases varied, depending on the nature of the DNA damaging agent and the cellular DNA repair background. We examined the role of Yap1 as a potential mediator of the DNA damage response by monitoring its subcellular localization following exposure to MMS in DNA repair proficient cells. We found that Yap1 relocalizes to the nucleus in response to MMS exposure and that this effect is similar to that seen with direct exposure to H_2O_2 . The activation of Yap1 in response to MMS further supports the idea that the increase in ROS in response to DNA damage may function in signaling processes.

Experimental Procedures

Strains, Media, and Growth Conditions

The set of isogenic *S. cerevisiae* strains used in this study was derived from wild type (WT) SJR751 (*MAT α ade2-101oc his3 Δ 200 ura3 Δ Nco lys2 Δ Bgl leu2-R*). The genotypes derived from SJR751 are BER- deficient strain SJR867 (*MAT α ade2-101oc his3 Δ 200 ura3 Δ Nco lys2 Δ Bgl leu2-R ntg1 Δ ::LEU2 ntg2 Δ ::hisG apn1D1 ::HIS3*), NER- deficient strain SJR868 (*MAT α ade2-101oc his3 Δ 200 ura3 Δ Nco lys2 Δ Bgl leu2-R rad1 Δ ::hisG*), and BER-/NER-deficient strain SJR1101 (*MAT α ade2-101oc his3 Δ 200 ura3 Δ Nco lys2 Δ Bgl leu2-R ntg1 Δ ::LEU2 ntg2 Δ ::hisG apn1D1 ::HIS3 rad1 Δ ::hisG*). All of the SJR derived strains were constructed as previously reported [24]. Yeast strains were grown on YPD media (1% yeast extract, 2% peptone, 2% dextrose and 2% agar for plates). All YPD media were supplemented with 0.5% adenine sulfate. For selection of strains containing the Yap1-GFP plasmid, the strains were grown on SD-minimal –URA media (0.5% ammonium sulfate, 0.17% yeast nitrogen base without amino acids, 2% dextrose, 0.14% minimal Ura drop out mix, and 2.5% agar for plates) [25].

Cell Growth and Viability

Liquid YPD media was inoculated with yeast cells and grown at 30 °C for ~24 hrs to a density greater than 7×10^7 cells/mL. The density of the cells was determined by counting on a hemacytometer. Fifty milliliters YPD cultures were inoculated with an appropriate amount of cells so that the culture would reach a density of 2×10^7 after 12 hrs of growth at 30 °C. Cell viability was determined by plating on YPD after exposure to MMS or UV-C. Cultures were diluted to a density that would yield approximately 100–200 colonies per plate. The data from six independent experiments was used to calculate the cytotoxicity in these strains.

YAP1-GFP Plasmid Construction

For studies of the subcellular localization of Yap1, WT strains were transformed with pLR1 plasmid. The pLR1 plasmid is a centromeric vector containing a *YAP1::GFP* fusion protein and a *URA3* marker. The plasmid was constructed using the “Drag&Drop” method of cloning [26]. The original pLDB419 plasmid is a *YAP1::GFP LEU2* 2 μ plasmid [21]. We amplified by PCR the *YAP1::GFP* DNA fragment from pLDB419 using the following primers. 5'-

CACTATAGGGCGAATTGGAGCTCCACCGCGGTGGCGGCCGCTCTAATGACCATG ATTACGAATTCGAGCT-3' and the reverse primer was 5'-GGGAACAAAAGCTGGGTACCGGGCCCCCCTCGAGGTCGACGGTCCAAGCTTCATG CCTGCAGGTCGT-3'. The sequences of these primers are homologous to the flanking sequences of *XbaI-XhoI* digested plasmid pRS306 [27]. Co-transformation of the WT strain with the *YAP1::GFP* containing PCR fragment and *XbaI-XhoI* digested plasmid pRS306 and following rescue of the plasmid yielded pLR1.

Measurement of Reactive Oxygen Species Levels

ROS subspecies ($O_2^{\bullet-}$, H_2O_2 , and $\bullet OH$) were detected using a panel of fluorescent probes. Cells were grown to mid-log ($\sim 2 \times 10^7$ cells/mL) in YPD at 30 °C overnight. Cells were counted (hemacytometer), washed twice in H_2O and then adjusted to 2×10^7 cells/mL in H_2O . Cells were then exposed to various doses of either UV-C or MMS. For experiments involving UV irradiation, cells (15 mL) were placed in a 15 mm petri dish and exposed to a range of UV-C doses (0–50 J/m²). Immediately after UV exposure, cells were placed in the dark to prevent photoreactivation. For experiments involving MMS, cells (3 mL) were placed in the dark and exposed to a range of MMS doses (0–55 mM) for 30 min at 30 °C. Following exposure to MMS or UV-C, 1 mL aliquots were plated for survival measurements and 2 mL were incubated with various fluorescent probes (Dihydrorhodamine (DHR), 25 μ g/mL; Dihydroethidium (DHEt), 50 μ g/mL; N-can-Acetyl-3,7-dihydroxy-phenoxazine (Amplex Red (APR)), 12 μ g/mL; and 2-[6-(4'-Hydroxyphenoxy-3H-xanthen-3-on-9-yl)] benzoic acid (HPF), 20 μ g/mL) for ROS measurements. Immediately following fluorescent probe addition, cells were held in the dark and incubated at 30 °C for 2 hrs. Cells were subsequently washed twice with H_2O and then resuspended in 2 mL phosphate buffered saline (PBS) and assessed for fluorescence intensity employing a BD™ LSR II flow cytometer (BD Biosciences). Approximately 10,000 cells were evaluated for fluorescence intensity (BD™ LSR II flow cytometer (BD Biosciences)) in three independent experiments.

Yap1 Cellular Localization Studies

Cells were grown to mid-log phase ($\sim 2 \times 10^7$ cells/mL) in YPD at 30 °C overnight, counted, and washed twice with H_2O , and then adjusted in H_2O to a density of 2×10^7 cells/mL. Cells were then stained with 4',6-diamidino-2-phenylindole (DAPI) (Invitrogen) to visualize DNA in nuclei and mitochondria. Cells were incubated with 1 μ L 100 nM DAPI/mL of cells for 5 min, washed once with H_2O , and then resuspended to the original volume in H_2O . Cells were then exposed to either H_2O_2 or MMS as described above. Cells were subjected to fluorescent confocal microscopy (Zeiss LSM510 META) and images were analyzed using the Carl Zeiss LSM Image Browser software. A minimum of 100 cells were counted for each time point in two independent experiments.

Results

In the present study, we used the budding yeast *S. cerevisiae*, as a model system to address whether cells exhibiting compromised DNA damage repair contain increased levels of ROS. Previously, we reported that unrepaired, endogenously generated oxidative DNA damage accumulates in cells deficient in both BER- (*ntg1Δ ntg2Δ apn1Δ* triple mutant) and NER- (*rad1Δ* mutants) (BER-/NER-) and is accompanied by an increase in intracellular ROS [9]. Despite the fact that Rad1p functions in homologous recombination, it mediates the relatively minor role of removing the heterologies during strand invasion and single strand annealing (reviewed in [28]). It was also reported after exposure to increasing doses of H_2O_2 , WT and BER-deficient cells contain an increasing number of Ntg1-recognized lesions per genome. For a given H_2O_2 dose, the level of Ntg1-recognized lesions is greater in BER-deficient cells compared to WT cells (Supplementary Table S1) [10]. At an exposure dose of 25mM H_2O_2 ,

WT cells contained 2240 lesions per genome and displayed a significant increase in the level of ROS in a subset of the cell population. At an exposure dose of 5 mM H₂O₂ BER-deficient cells display a similar number (2820) of lesions per genome and also display a similar increase in the level of ROS in a subset of the population (Supplementary Figure S1) [9,10]. These results taken together reveal a correlation between the amount of DNA damage present in the genome and the levels of ROS being produced in WT and BER-deficient cell. These studies suggested that even non-toxic or moderately toxic DNA damage might be capable of mediating the ROS response. However, the specific types of ROS involved were not identified due to the utilization of DHR, a fluorescent probe that detects multiple ROS species including H₂O₂, •OH, and NO• [29,30].

Two major objectives of the present study were (i) to determine whether the ROS response could be elicited by different classes of DNA damaging agents, thus implicating a role for ROS in a general genotoxic stress response and (ii) to define the nature of the stress response with respect to individual types of ROS induced by different classes of DNA damage. Taking into account that cell death could cause the release of ROS [31,32], we first defined the cytotoxicity profiles for MMS and UV-C in cells defective in different repair pathways.

Cytotoxicity of MMS and UV-C in Yeast Strains with Different DNA Repair Backgrounds

To delineate the potential relationship between DNA damage-induced cell death and intracellular ROS levels, dose dependent cytotoxicity profiles were determined for isogenic strains with different DNA repair deficiencies (WT, BER-, NER-, and BER-/NER-) exposed to MMS or UV-C. MMS induces several different alkylation base damage products that are primarily repaired by BER [33]. Thus, it could be expected that BER- deficient cells should exhibit the greatest cytotoxicity in response to MMS exposure. Cells were exposed to a range of doses (0–55 mM) of MMS and the cytotoxicity was determined. Severely repair-deficient cells (BER-/NER-) exhibit a moderate (35%) decrease in survival upon exposure to low doses (0.5 mM) of MMS and exhibited extreme sensitivity to higher doses (Fig. 1 A). In contrast, for repair-proficient strains (WT) and single pathway-compromised (BER- deficient and NER-deficient) strains, significant decreases in survival are observed only with exposure to doses above 5 mM MMS. At such higher MMS doses, the single pathway-deficient mutants (BER- or NER-) displayed greater sensitivity than repair-proficient cells (WT), with BER-deficient strains exhibiting greater sensitivity compared to NER-deficient strains. Thus, as might be expected, MMS sensitivity is variable depending on the DNA repair capacity of the cells, with cells deficient in BER alone or in combination with NER displaying the greatest sensitivity.

Short wavelength ultraviolet radiation (UV-C) induces toxic, mutagenic bipyrimidine photoproducts that are repaired primarily by the NER pathway [34]. Cells were exposed to a range of doses (0–50 J/m²) of UV-C and the cytotoxicity was determined. As expected, repair proficient (WT) and BER-deficient cells exhibited similar sensitivities to UV-C with NER- and BER-/NER-deficient strains displaying extreme sensitivity (less than 1% survival) at lower doses (5 J/m²) (Fig. 1 B). These experiments established a cytotoxicity profile for MMS and UV-C for each isogenic strain harboring DNA damages primarily repaired by BER or NER, respectively. Such profiles were then utilized to determine whether DNA damage-induced cytotoxicity was directly related to DNA damage-induced increases in intracellular ROS levels.

Endogenous DNA Damage and Intracellular ROS Levels in DNA Repair Compromised Strains

To determine the levels of individual types of ROS, WT, BER-, NER-, and BER-/NER-deficient strains were analyzed using a panel of fluorescent probes including DHR, DHEt, HPF, and APR. These probes detect different, specific subspecies of ROS. As discussed above, DHR is a relatively non-specific probe as it will detect a variety of ROS subspecies [29,30]. In contrast, DHEt is specific for O₂^{•-} [35,36], APR is specific for H₂O₂ [37,38], and HPF is

specific for $\cdot\text{OH}$ [39]. Cells treated with DHR (Fig. 2 A) revealed that ROS levels (multiple species) were significantly increased (approximately 30%) in the BER-/NER- deficient cells compared to repair proficient cells (WT). However, with this probe there was no increase observed in the strains deficient in either BER or NER pathways alone. A similar result was obtained when cells were incubated with the $\cdot\text{OH}$ -specific probe HPF (Fig. 2 C). When the levels of $\text{O}_2^{\cdot-}$ were determined with DHEt (Fig. 2 B), small to moderate increases were observed in both BER-deficient (~33% increase) and NER-deficient (~4% increase) cells, and a substantial (~80% increase) increase was observed in BER-/NER-deficient cells. These findings are consistent with previous studies employing DHR [9] but also reveal the nature of the specific types of ROS elevated in response to endogenously produced DNA damage in the absence of exposure to exogenous agents (Experimental Procedures). Only BER-/NER-deficient cells showed any significant increase in H_2O_2 when probed with APR (Fig. 2 D), and interestingly, a 30% decrease in H_2O_2 was observed in the NER- deficient strain. Currently, we cannot account for the observed decrease in H_2O_2 in NER-deficient cells. In general, when cells are severely repair-deficient and therefore accumulating endogenous DNA damage, there is a substantial increase in ROS levels. We conclude from these experiments that cells harboring elevated levels of endogenous DNA damage (BER-/NER-) have increased intracellular levels of $\text{O}_2^{\cdot-}$, H_2O_2 , and $\cdot\text{OH}$.

The finding that cells deficient in the repair of endogenous DNA damage (particularly BER-/NER-) contained elevated levels of oxidative damage that correlate with an elevation of ROS suggested that DNA damage induced by exogenous chemical and physical agents might be capable of causing a similar ROS response [9]. We addressed whether different classes of DNA damage, repaired by different DNA repair pathways were capable of eliciting an increase in ROS by examining the response to MMS, which produces DNA damage primarily repaired by BER and UV-C, which produces DNA damage primarily repaired by NER [19].

MMS Induced DNA Damage Causes an Increase in Intracellular ROS

First, we examined the spectrum of ROS produced in the repair deficient strains in response to MMS. All four strains (WT, BER-, NER-, and BER-/NER-) were exposed to a range (non-toxic to toxic) of MMS doses (0–55 mM) for 30 min and then assessed for ROS using the fluorescent probes described in Experimental Procedures. When cells were exposed to MMS and then treated with DHR (Fig. 3B) or DHEt (Fig. 3C), an increase in ROS is observed that is related to the exposure dose. There is a significant increase in the levels of ROS in response to MMS (25 mM) in all strains irrespective of the DNA repair background and the corresponding level of cytotoxicity caused by this dose. The observed increases in ROS range from 15–2500% depending on the probe employed and the strain analyzed. In general, the increases in ROS are related to an expected increase in DNA damage and not cytotoxicity (Fig. 3A). The cytotoxicity observed following a 0.5 mM MMS exposure dose is similar in all four strains while the levels of intracellular $\text{OH}\cdot$ and H_2O_2 (Fig. 3 D, E) differ significantly. In WT and NER- deficient cells, there is no significant change in the levels of $\cdot\text{OH}$ and H_2O_2 . However, in BER-deficient cells there is a 18% and 8% increase (indicated with “*” in Fig. 3 D,E) in $\cdot\text{OH}$ and H_2O_2 , respectively and in BER-/NER-deficient cells a 36% and 41% increase (indicated with “#” in Fig. 3 D,E) in $\cdot\text{OH}$ and H_2O_2 , respectively.

When cells were probed with HPF (Fig. 3 D) or APR (Fig. 3 E), an increase in $\cdot\text{OH}$ and H_2O_2 , respectively, is observed at lower exposure doses of MMS (0.5 mM or 5 mM) followed by a decrease at the higher doses (25 mM and/or 55 mM MMS). This increase is observed at 0.5 mM MMS for BER- deficient cells (18% and 8% increases with HPF and APR, respectively) and BER-/NER-deficient cells (36% and 41% increases with HPF and APR, respectively). A similar increase is not observed in WT and NER- deficient cells until higher exposure doses (5 mM) of MMS are used. The decrease in the levels of different ROS

subspecies occurs at different doses of MMS in most strains. Unlike the decrease in $\cdot\text{OH}$ that is observed at higher MMS doses, (Fig. 3 D), the decrease in H_2O_2 observed with APR (Fig. 3 E) was observed at a 25 mM MMS exposure dose in BER- and BER-/NER-deficient cells and 55 mM MMS in WT and NER- deficient cells. The trend that the levels of H_2O_2 and $\cdot\text{OH}$ increase at lower exposure doses of MMS followed by a decrease at higher doses is observed for most strains investigated with one exception (BER-/NER- deficient cells).

UV Light Induced DNA Damage Causes an Increase in Intracellular ROS

Exposure of cells to MMS reveals a potential role for ROS in the cellular response to a DNA alkylating agent. As previously reported with the nonspecific probe DHR., there is an increase in ROS in several DNA repair deficient strains in response to H_2O_2 and MMS exposure [10].

An important issue in the present study was to determine whether or not the increase in ROS in response to DNA damage repaired by BER is also observed for DNA lesions primarily repaired by the other major excision repair pathway, NER. To address this possibility, we determined the levels of ROS in response to UV-C induced DNA damage. Unlike MMS and H_2O_2 , UV-C produces helix-distorting bipyrimidine adducts (CPDs and 6-4 PPs) that are repaired by NER [19].

All four strains (WT, BER-, NER-, and BER-/NER-) were exposed to a range (non-toxic to toxic) of doses (0–50 J/m^2) of UV-C and then probed for ROS. A pattern of a dose-dependent increase in ROS levels similar to that obtained with MMS exposure was observed. However, the maximum relative levels of ROS detected following exposure to UV-C (Fig. 4 B,C) were lower than that observed for MMS (Fig. 3 B,C). As with MMS, the observed increase in $\text{O}_2^{\cdot-}$ is directly related to the UV exposure dose (Fig. 4 C). There is a significant increase in the levels of $\text{O}_2^{\cdot-}$ in response to 5 J/m^2 UV-C in all strains (ranging from 14–30%) as compared to the levels of ROS in unexposed cells (indicated with “*” in Fig. 4C). These results are similar to those observed in cells following exposure to MMS in that there is a dose-dependent increase in the levels of ROS in response to DNA damage. Furthermore, NER- deficient strains are more sensitive to UV-C induced DNA damage at lower doses. NER- deficient cells also exhibited a significant increase in $\text{O}_2^{\cdot-}$, but at a lower dose (2 J/m^2) as compared to unexposed (indicated with “#” in Fig. 4C).

As in the case of MMS exposure, exposure to UV-C results in changes in ROS levels that are related to an expected increase in DNA damage and not cell death. When cells are exposed to 25 J/m^2 UV-C, there is a greater than 50% survival in both the WT and BER- deficient cells while there is less than 1% survival in NER- and BER-/NER- deficient cells (Fig. 4 A). Despite substantial differences in survival, these cells display similar relative increases in the levels of $\text{O}_2^{\cdot-}$ in response to 25 J/m^2 UV-C (Fig. 4 C). The fact that these increased levels of ROS are not associated with cell death is also revealed when cells are probed with HPF. For example, BER-deficient cells exposed to 50 J/m^2 UV-C and NER-deficient cells exposed to 5 J/m^2 UV-C display similar survival yet have significantly different levels of OH^{\cdot} (indicated with “‡” in Fig. 4D).

It is important to emphasize that when cells were probed with DHR (Fig. 4 B), a difference was observed between cells capable of repairing UV-C-induced damage (WT and BER-deficient), and cells that are not capable of repairing such DNA damage (NER- and BER-/NER-deficient). NER- and BER-/NER-deficient cells exhibited a significant (compared to unexposed cells in the corresponding strain) increase (indicated with “†” in Fig. 4 B) in ROS at lower doses (2 and 5 J/m^2) and a decrease in ROS at higher, more toxic doses (25 and 50 J/m^2). As with MMS, we observed an increase in $\cdot\text{OH}$ and H_2O_2 at lower doses (5–25 J/m^2) of UV-C and a decrease in $\cdot\text{OH}$ and H_2O_2 at higher doses (25–50 J/m^2) of UV-C (Fig 4D–E). We conclude that cells respond to DNA damage through changes in the types and levels of ROS

produced. As discussed below, the biological relevancy of an apparently bimodal ROS response to DNA damage is likely to involve specific signal transduction pathways.

Yap1 Relocalization in Response to DNA Damage

Under normal cellular environments, the ROS sensor and transcription factor, Yap1 is rapidly exported from the nucleus to the cytoplasm where it resides until activated in response to oxidative stress [14,16,21,22]. Upon activation, Yap1 can no longer bind to the nuclear export receptor Crm1p and thus accumulates in the nucleus where it functions as a transcription factor [22,23,40]. Previous reports have shown that H₂O₂ exposure causes Yap1 to rapidly relocalize to the nucleus [14]. To address the potential role of Yap1 in the ROS-mediated DNA damage response, the localization of Yap1 was determined following exposure to MMS and compared to the previously characterized effects caused by direct exposure to H₂O₂ [14,21]. Cells were exposed to a range of non-toxic to toxic doses of H₂O₂ or MMS for 1 hr and the localization of Yap1-GFP was determined by direct fluorescence microscopy. Following exposure to H₂O₂, DNA repair proficient (WT) cells exhibited a rapid relocalization of Yap1 to the nucleus that was maintained for at least 60 min. On average, approximately 75% of the cells analyzed exhibited nuclear localization of Yap1 (Fig. 5). WT cells exposed to a range (0.5–55 mM) of MMS doses displayed a delay in relocalization of Yap1 to the nucleus compared to the relocalization pattern observed following exposure to H₂O₂ (Fig. 6). When WT cells were exposed to 0.5 mM MMS, fewer than 20% of the cells displayed nuclear localization of Yap1 throughout the time course (60 min) of the experiment (Fig. 6 B). However with higher doses (25 and 55 mM) of MMS Yap1 nuclear localization significantly increased (up to 60%), indicating a response to oxidative stress that occurs after the introduction of non-oxidative DNA damage into the genome (Fig. 6 C,D).

Discussion

By examining the levels of ROS in cells harboring DNA damage caused by endogenous or exogenous sources, insight can be gained into the nature of genotoxic stress responses. DNA damage occurs continuously in all cells. Multiple overlapping systems for handling DNA damage exist. However, deleterious consequences can result when such pathways are compromised or when their capacities to process DNA damage have been exceeded. Although increases in ROS levels are thought to be involved in numerous pathological states, it is clear that modulation of ROS is also important for normal cellular physiology [41].

The endogenous levels of several different types of ROS were determined for WT and DNA repair deficient yeast strains. These strains were previously evaluated for the levels of endogenous oxidative DNA damage [9]. An increase in oxidative DNA damage in BER- and BER-/NER- deficient strains was observed and was found to be highest in the BER-/NER- deficient strain. The results presented in the current study, establish a relationship between the levels of accumulated oxidative DNA damage and the levels of various ROS subtypes. We showed that BER-/NER- deficient cells harboring increased levels of oxidative DNA damage displayed the highest levels of intracellular O₂^{•-} as well as increased levels of intracellular H₂O₂ and [•]OH. BER- deficient cells exhibited an increase in oxidative DNA damage that is less than that observed in BER-/NER- deficient cells. BER- deficient cells exhibit a correspondingly smaller increase in O₂^{•-} with no observed increase in either H₂O₂ or [•]OH as compared to BER-/NER- deficient cells (Fig. 2). NER-deficient cells show no detectable increases in the levels of oxidative DNA damage and exhibit a very small increase in the levels of O₂^{•-} and no increases in the other types of ROS. Thus, low levels of endogenous DNA damage causes production of O₂^{•-}. As the levels of endogenous DNA damage increase, O₂^{•-} also increases with concomitant elevation in both H₂O₂ and [•]OH.

In this study, by utilizing two different classes of DNA damaging agents (MMS and UV-C), we were able to determine the response to damage that is primarily repaired by either BER or NER. When cells were exposed to either MMS or UV-C, an increase in three different subspecies of ROS was observed, as a general genotoxic stress response regardless of the nature of the damage.

Previous reports have suggested that increased levels of ROS are associated with cell death [31],[32]. Our results indicate that ROS increases are also associated with DNA damage that occurs following non-toxic to moderately toxic exposure to MMS or UV light. Thus elevated levels of ROS cannot be attributed solely to cell death. For example, the cytotoxicity resulting from a low dose (0.5 mM) MMS exposure is similar in all strains (70–98% survival), but the levels of intracellular H₂O₂ produced are significantly different for BER- and BER-/NER-deficient cells (8% and 41% increases, respectively) while there was no change in intracellular ROS levels for WT or NER- deficient cells (Fig. 3). DNA damage produced by MMS is primarily repaired by BER and accumulation of base damage would be expected in BER- and BER-/NER- deficient strains. We have established that there is a substantial increase in the levels of H₂O₂ without significant changes in cell survival. These results confirm the notion that ROS is produced directly in response to DNA damage and is not due to cell death.

Redox homeostasis in cells is important for maintaining proper cellular functions [42]. Elevated levels of ROS can be biologically deleterious, but have also been implicated in a variety of cell signaling processes [5–8]. For example, ROS alter protein structure through direct interaction with cysteinyl sulfhydryl groups [7]. To maintain normal redox states, cells utilize several systems for buffering ROS including the thioredoxin and glutathione pathways [43]. In dividing cell populations, when DNA damage occurs, the cell must respond to maintain the integrity of the genome and eventually continue through the cell cycle. ROS-mediated signaling should enable the rapid activation of the stress response systems necessary for cell survival. To our knowledge, this is the first report defining the relationship between DNA damage and the types and relative levels of ROS produced.

To further delineate the possible role of ROS in the DNA damage response, the localization of the ROS sensor, Yap1 in WT cells in response to two different DNA damaging agents was examined. Previously Yap1 has been shown to relocalize to the nucleus in response to H₂O₂. Yap1 localization is directly altered by the presence of H₂O₂ in the cell [13,21], regardless of its DNA damage effect. In this study, we found that the relocalization of Yap1 in response to MMS exposure is similar to the relocalization of Yap1 as a result of direct exposure to ROS (e.g. H₂O₂). When cells are exposed to MMS, there is a time- and dose-dependent increase in the number of cells that have predominantly nuclear Yap1 localization. However, unlike the response observed, after exposure to H₂O₂, of rapid relocalization of Yap1 to the nucleus, there is a delay of approximately 25 min before a significant number of MMS-exposed cells contain nuclear Yap1 (Fig. 6). As the redox state of the cell shifts to a more reduced state through the increased production of ROS in response to DNA damage, the localization of Yap1 changes from cytoplasmic to nuclear where it functions as a transcription factor in response to cell stress. It should be emphasized that MMS, does not directly produce ROS, yet causes the accumulation of Yap1 in the nucleus as does H₂O₂. This observation provides independent verification that DNA damage per se elicits the ROS stress response. The delayed accumulation of Yap1 in the nucleus following MMS exposure suggests a signal transduction process from DNA damage to the generation of ROS. These observations provide biological confirmation of the DNA damage-induced intracellular ROS production revealed by the panel of fluorescent probes employed in these studies.

Our results are consistent with the following model for the role of ROS in the cellular genotoxic stress response (Fig. 7). Elevation of ROS in response to DNA damage appears to be associated

with two modes of DNA damage levels involving $O_2^{\bullet-}$ as the primary mediator. At low to moderate levels of DNA damage, there is a moderate increase in the levels of $O_2^{\bullet-}$, H_2O_2 , and $\bullet OH$ (Level 1). At Level 1, $O_2^{\bullet-}$ is a likely source for H_2O_2 and $\bullet OH$ through chemical and enzymatic conversion pathways [44]. For example, $\bullet OH$ can be non-enzymatically generated via the Fenton Reaction and H_2O_2 can be enzymatically produced by superoxide dismutase [44]. The redox state (Mode 1) of the cell at these levels of DNA damage leads to cell survival-related and stress response signaling processes. In response to changes in cellular redox states, there are several known signaling pathways that can be activated including stress activated kinases (SAPKs), multistep phosphorelay, and AP-1 like transcription factor sensing [45]. In addition, several conserved sequences (antioxidant response elements, ARE [46], and stress response elements, StRE [47]) are found in the promoter region of many genes and are activated in response to stress. These pathways are conserved between yeast and other higher organisms, making these studies potentially relevant to other eukaryotes. Activating protein-1 (AP-1)-like transcription factor sensing is mediated by a family of transcription factors. AP-1-like proteins regulate a variety of cellular processes including proliferation, differentiation, apoptosis, and various stress responses [48]. In *S. cerevisiae* Yap1 is the major AP-1-like transcription factor. Yap1 is responsible for the up regulation of numerous genes that are involved in the oxidative stress response. These include the glutathione reductase (*GLR1*), thioredoxin (*TRX2*), catalase (*CTT1*), and superoxide dismutase (*SOD1*) [49]. It is possible that the DNA damage stress response in *S. cerevisiae* may be initiated by changes in the redox state of the cell that, in turn, can lead to subsequent signaling through one or more of the above pathways. Many of these pathways may contain components that sense intracellular ROS levels and then initiate events that trigger a stress response in cells. A Mode 1 response could be mediated by activated Yap1 as we have demonstrated that it accumulates in the nucleus following exposure to MMS.

At high levels of DNA damage, there is a corresponding increase in the level of $O_2^{\bullet-}$, but not in H_2O_2 or $\bullet OH$ due to saturation or blockage of conversion pathways. With such decreases in H_2O_2 or $\bullet OH$ the appropriate signaling response does not occur, thus leading to a decrease in cell survival. At the corresponding redox state (Mode 2), the cell is well beyond its repair capacity and reorchestrates signaling from cell survival/stress responses to cell death processes.

As the redox state of the cell continues to move towards an oxidized state due to high levels of DNA damage causing an increase in the levels of $O_2^{\bullet-}$, the cell can no longer survive because of extensive nuclear and/or mitochondrial DNA damage as well as damage to other macromolecules. Alternatively, the cell reorchestrates the internal signaling processes to initiate cell death. Several recent studies have shown that unicellular eukaryotes undergo a caspase-independent apoptotic-like cell death process [50,51]. In yeast, many features of apoptosis have been observed including chromatin condensation, phosphatidylserine exposure on the outer membrane, and cytoplasmic shrinkage [50,52]. Importantly, one feature of this cell death process is an increase in the intracellular levels of $O_2^{\bullet-}$ [31].

To fully understand how the DNA damage-induced stress response functions in cells, an understanding of the generators of ROS and their role in the ROS response is necessary. There are several possible $O_2^{\bullet-}$ generators that have been identified in yeast cells including the mitochondria (e.g. cytochrome C) and various oxidases. Xanthine oxidase is an interesting candidate in that it has been shown to produce $O_2^{\bullet-}$, H_2O_2 , and $\bullet OH$ [53]. Other candidates such as NADPH oxidases [54,55] are present in mammalian cells, but not *S. cerevisiae*. In addition, we are currently determining the extent to which a similar DNA damage-induced ROS stress response occurs in mammalian cells. Such a response has obvious implications for several important human pathologies, including cancer.

Supplementary Material

Refer to Web version on PubMed Central for supplementary material.

Acknowledgements

We would like to thank Myfanwy Hopkins for her assistance with some of the experiments. We also thank Dr. Katherine Hales and Dr. Adam Marcus and the Cell Imaging and Microscopy Core of the Emory Winship Cancer Institute for assistance with the microscopy experiments and Dr. Robert Karaffa and The Emory University School of Medicine Core Facility for Flow Cytometry for their assistance with the flow cytometry experiments. We also thank Dr. Anita Corbett for plasmids, helpful discussions and critical reading of the manuscript. This work was supported by NIH Grant ES 011163 (PWD).

Abbreviations used in text

ROS, Reactive oxygen species
 BER, Base excision repair
 NER, Nucleotide excision repair
 MMR, Mismatch repair
 TLS, Translesion synthesis
 REC, Recombination
 CPD, Cyclobutane pyrimidine dimer
 6-4 PP, 6-4 photoproduct
 H₂O₂, Hydrogen peroxide
 MMS, methyl methanesulfonate
 O₂^{•-}, Superoxide
 •OH, Hydroxyl radical
 UV-C, Short wavelength ultraviolet light
 WT, Wild type
 DHR, Dihydrorhodamine
 DHEt, Dihydroethidium
 HPF, 2-[6-(4'-Hydroxy)phenoxy-3H-xanthen-3-on09yl]
 APR, N-can-Acetyl-3,7dihydroxyphenoxazine (Amplex Red)
 PBS, Phosphate buffered saline
 DAPI, 4',6-diamidino-2-phenylindole
 SAPK, Stress activated kinases
 MAPK, Mitogen-activated protein kinases
 AP-1, Activating protein-1

References

1. Droge W. Free Radicals in the Physiological Control of Cell Function. *Physiological Reviews* 2002;82:47–95. [PubMed: 11773609]
2. Alexander RW. Hypertension and the Pathogenesis of Atherosclerosis : Oxidative Stress and the Mediation of Arterial Inflammatory Response: A New Perspective. *Hypertension* 1995;25:155–161. [PubMed: 7843763]
3. Dreher D, Junod A. Role of Oxygen Free Radicals in Cancer Development. *European Journal of Cancer* 1996;32A:30–38. [PubMed: 8695238]
4. Harman D. The Aging Process. *Proc Natl Acad Sci* 1981;78:7124–7128. [PubMed: 6947277]
5. Genestra M. Oxyl radicals, redox-sensitive signalling cascades and antioxidants. *Cellular Signalling* 2007;19:1807–1819. [PubMed: 17570640]
6. Kamata H, Hirata H. Redox Regulation of Cellular Signalling. *Cellular Signalling* 1999;11:1–14. [PubMed: 10206339]

7. D'Autreaux B, Toledano MB. ROS as signalling molecules: mechanisms that generate specificity in ROS homeostasis. *Nature Reviews Molecular Cell Biology* 2007;8:813–824.
8. Apel K, Hirt H. Reactive Oxygen Species: Metabolism, Oxidative Stress, and Signal Transduction. *Annual Review of Plant Biology* 2004;55:373–399.
9. Evert BA, Salmon TB, Song B, Jingjing L, Siede W, Doetsch PW. Spontaneous DNA Damage in *Saccharomyces cerevisiae* Elicits Phenotypic Properties Similar to Cancer Cells. *The Journal of Biological Chemistry* 2004;279:22585–22594. [PubMed: 15020594]
10. Salmon TB, Evert BA, Song B, Doetsch PW. Biological consequences of oxidative stress-induced DNA damage in *Saccharomyces cerevisiae*. *Nucleic Acids Research* 2004;32:3712–3723. [PubMed: 15254273]
11. Begley TJ, Samson LD. Network responses to DNA damaging agents. *DNA Repair* 2004;3:1123–1132. [PubMed: 15279801]
12. Fry RC, Begley TJ, Samson LD. Genome-Wide Responses to DNA-Damaging Agents. *Annual Review of Microbiology* 2005;59:357–377.
13. Delaunay A, Isnard A-D, Toledano MB. H₂O₂ sensing through oxidation of the Yap1 transcription factor. *The EMBO Journal* 2000;19:5157–5166. [PubMed: 11013218]
14. Delaunay A, Pflieger D, Barrault M-B, Vinh J, Toledano MB. A Thiol Peroxidase Is an H₂O₂ Receptor and Redox-Transducer in Gene Activation. *Cell* 2002;111:471–481. [PubMed: 12437921]
15. Moye-Rowley WS, Harshman KD, Parker CS. Yeast YAP1 encodes a novel form of the jun family of transcriptional activator proteins. *Genes and Development* 1989;3:283–292. [PubMed: 2542125]
16. Rodrigues-Pousada CA, Nevitt T, Menezes R, Azevedo D, Pereira J, Amaral C. Yeast activator proteins and stress response: an overview. *FEBS Letters* 2004;567:80–85. [PubMed: 15165897]
17. Coleman ST, Epping EA, Steggerda SM, Moye-Rowley WS. Yap1p Activates Gene Transcription in an Oxidant-Specific Fashion. *Molecular and Cellular Biology* 1999;19:8302–8313. [PubMed: 10567555]
18. Friedberg, EC.; Walker, GC.; Siede, W.; Wood, RD.; Schultz, RA.; Ellenberger, T. *DNA Repair and Mutagenesis*. Washington, DC: ASM press; 2006.
19. Lindahl T, Wood RD. Quality Control by DNA Repair. *Science* 1999;286:1897–1905. [PubMed: 10583946]
20. Jamieson DJ. Oxidative stress responses of the yeast *Saccharomyces cerevisiae*. *Yeast* 1998;14:1511–1527. [PubMed: 9885153]
21. Yan C, Lee LH, Davis LI. Crm1p mediates regulated nuclear export of a yeast AP-1-like transcription factor. *The EMBO Journal* 1998;17:7416–7429. [PubMed: 9857197]
22. Kuge S, Jones N, Nomoto A. Regulation of yAP-1 nuclear localization in response to oxidative stress. *The EMBO Journal* 1997;16:1710–1720. [PubMed: 9130715]
23. Kuge S, Jones N. YAP1 dependent activation of TRX2 is essential for the response of *Saccharomyces cerevisiae* to oxidative stress by hydroperoxides. *The EMBO Journal* 1994;13:655–664. [PubMed: 8313910]
24. Swanson RL, Morey NJ, Doetsch PW, Jinks-Robertson S. Overlapping Specificities of Base Excision Repair, Nucleotide Excision Repair, Recombination, and Translesion Synthesis Pathways for DNA Base Damage in *Saccharomyces cerevisiae*. *Molecular and Cellular Biology* 1999;19:2929–2935. [PubMed: 10082560]
25. Guthrie C, Fink G. *Guide to Yeast Genetics and Molecular Biology*. *Methods in Enzymology* 1991;194
26. Jansen G, Wu C, Schade B, Thomas DY, Whiteway M. Drag&Drop cloning in yeast. *Gene* 2005;344:43–51. [PubMed: 15656971]
27. Sikorski RS, Hieter P. A System of Shuttle Vectors and Yeast Host Strains Designed for Efficient Manipulation of DNA in *Saccharomyces cerevisiae*. *Genetics* 1989;122:19–27. [PubMed: 2659436]
28. Symington LS. Role of RAD52 Epistasis Group Genes in Homologous Recombination and Double-Strand Break Repair. *Microbiol. Mol. Biol. Rev* 2002;66:630–670. [PubMed: 12456786]
29. Crow JP. Dichlorodihydrofluorescein and Dihydrorhodamine 123 Are Sensitive Indicators of Peroxynitrite In Vitro: Implications for Intracellular Measurement of Reactive Nitrogen and Oxygen Species. *Nitric Oxide* 1997;1:145–157. [PubMed: 9701053]

30. Royall JA, Ischiropoulos H. Evaluation of 2'-dichlorofluorescein and Dihydrorhodamine 123 as Fluorescent Probes for Intracellular H₂O₂ in cultured Endothelial Cells. *Archives of Biochemistry and Biophysics* 1993;302:348–355. [PubMed: 8387741]
31. Simon H-U, Haj-Yehia A, Levi-Schaffer F. Role of reactive oxygen species (ROS) in apoptosis induction. *Apoptosis* 2002;5:415–418. [PubMed: 11256882]
32. Eisenberg T, Büttner S, Kroemer G, Madeo F. The mitochondrial pathway in yeast apoptosis. *Apoptosis* 2007;12:1011–1023. [PubMed: 17453165]
33. Memisoglu A, Samson L. Base excision repair in yeast and mammals. *Mutation Research/ Fundamental and Molecular Mechanisms of Mutagenesis* 2000;451:39–51.
34. Costa RMA, Chigancas V, da Silva Galhardo R, Carvalho H, Menck CFM. The eukaryotic nucleotide excision repair pathway. *Biochimie* 2003;85:1083–1099. [PubMed: 14726015]
35. Benov L, Szejnberg L, Fridovich I. Critical Evaluation of the Use of Hydroetidine as a Measure of Superoxide Anion Radical. *Free Radical Biology & Medicine* 1998;25:826–831. [PubMed: 9823548]
36. Carter WO, Narayanan PK, Robinson JP. Intracellular hydrogen peroxide and superoxide anion detection in endothelial cells. *The Journal of Leukocyte Biology* 1994;55:253–258.
37. Mohanty JG, Jaffe JS, Schulman ES, Raible DG. A highly sensitive fluorescent micro-assay of H₂O₂ release from activated human leukocytes using a dihydroxyphenoxazine derivative. *Journal of Immunological Methods* 1997;202:133–141. [PubMed: 9107302]
38. Zhou M, Diwu Z, Panchuk-Voloshina N, Haugland RP. A Stable Nonfluorescent Derivative of Resorufin for the Fluorometric Determination of Trace Hydrogen Peroxide: Applications in Detecting the Activity of Phagocyte NADPH Oxidase and Other Oxidases. *Analytical Biochemistry* 1997;253:162–168. [PubMed: 9367498]
39. Setskunai, K-i; Urano, Y.; Kakinuma, K.; Majima, HJ.; Nagano, T. Development of Novel Fluorescence Probes That Can Reliably Detect Reactive Oxygen Species and Distinguish Specific Species. *The Journal of Biological Chemistry* 2003;278:3170–3175. [PubMed: 12419811]
40. Kuge S, Toda T, Iizuka N, Nomoto A. Crm1 (Xpo1) dependent nuclear export of the budding yeast transcription factor yAP-1 is sensitive to oxidative stress. *Genes to Cells* 1998;3:521–532. [PubMed: 9797454]
41. Finkel T, Holbrook NJ. Oxidants, oxidative stress and the biology of ageing. *Nature* 2000;408:239–247. [PubMed: 11089981]
42. Adler V, Yin Z, Tew KD, Ronai Z. Role of redox potential and reactive oxygen species in stress signaling. *Oncogene* 1999;18:6104–6111. [PubMed: 10557101]
43. Moradas-Ferreira P, Costa V. Adaptive response of the yeast *Saccharomyces cerevisiae* to reactive oxygen species: defences, damage and death. *Redox Report* 2000;5:277–285. [PubMed: 11145102]
44. Valko M, Rhodes CJ, Moncol J, Izakovic M, Mazur M. Free radicals, metals and antioxidants in oxidative stress-induced cancer. *Chemico-Biological Interactions* 2006;160:1–40. [PubMed: 16430879]
45. Ikner A, Shiozaki K. Yeast signaling pathways in the oxidative stress response. *Mutation Research/ Fundamental and Molecular Mechanisms of Mutagenesis* 2005;565:13–27.
46. Rushmore TH, Morton MR, Pickett CB. The Antioxidant Responsive Element. Activation by Oxidative Stress and Identification of the DNA Consensus Sequence Required for Functional Activity. *The Journal of Biological Chemistry* 1991;266:11632–11639. [PubMed: 1646813]
47. Treger JM, Thomas MR, McEntee K. Functional Analysis of the Stress Response Element and Its Role in the Multistress Response of *Saccharomyces cerevisiae*. *Biochemical and Biophysical Research Communications* 1998;243:13–19. [PubMed: 9473471]
48. Karin M, Liu Z, Zandi E. AP-1 function and regulation. *Current Opinions in Cell Biology* 1997;9:240–246.
49. Temple MD, Perrone GG, Dawes IW. Complex cellular responses to reactive oxygen species. *Trends in Cell Biology* 2005;15:319–326. [PubMed: 15953550]
50. Burhans WC, Weinberger M, Marchetti MA, Ramachandran L, D'Urso G, Huberman JA. Apoptosis-like yeast cell death in response to DNA damage and replication defects. *Mutation Research/ Fundamental and Molecular Mechanisms of Mutagenesis* 2003;532:227–243.

51. Madeo F, Engelhardt S, Herker E, Lehmann N, Maldener C, Proksch A, Wissing S, Fröhlich K-U. Apoptosis in yeast: a new model system with applications in cell biology and medicine. *Current Genetics* 2002;41:208–216. [PubMed: 12172961]
52. Madeo F, Frohlich E, Frohlich K-U. A Yeast Mutant Showing Diagnostic Markers of Early and Late Apoptosis. *The Journal of Cell Biology* 1997;139:729–734. [PubMed: 9348289]
53. Harris CM, Massey V. The Reaction of Reduced Xanthine Dehydrogenase with Molecular Oxygen. Reaction Kinetics and Measurement of Superoxide Radical. *The Journal of Biological Chemistry* 1997;272:8370–8379. [PubMed: 9079661]
54. Lambeth JD. NOX enzymes and the biology of reactive oxygen. *Nature Reviews. Immunology* 2004;4:181–189.
55. Lambeth JD. Nox/Duox family of nicotinamide adenine dinucleotide (phosphate) oxidases. *Current Opinion in Hematology* 2002;9:11–17. [PubMed: 11753072]

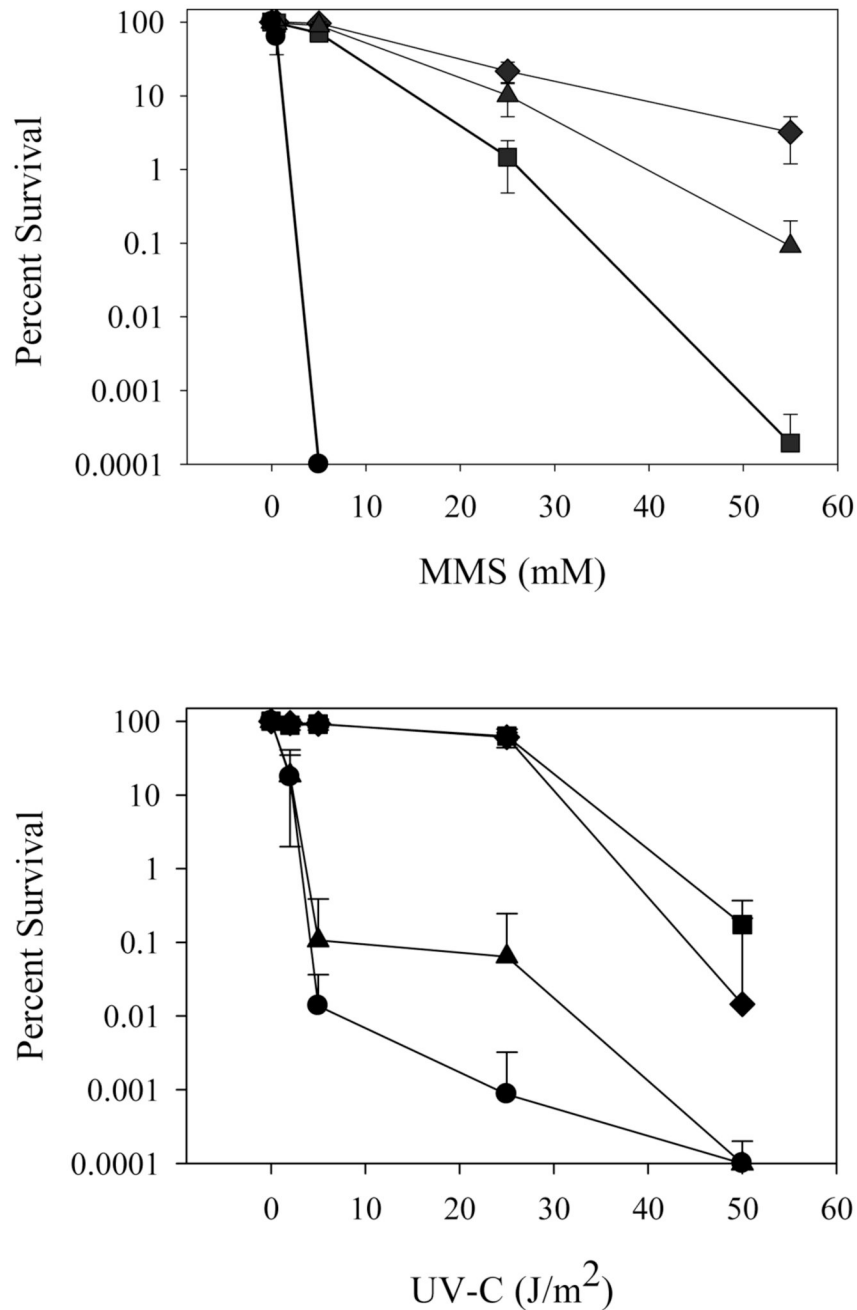


Figure 1. MMS and UV-C cytotoxicity profiles of cells with different DNA repair capacities
Sensitivity of DNA repair deficient strains to MMS and UV-C. WT (diamonds), BER- (squares), NER- (triangles), and BER-/NER- (circles). Cells were exposed to (A) 0, 0.5, 5, 25, and 55 mM MMS for 30 min at 30 °C or (B) 0, 2, 5, 25, 50 J/m² UV-C. The results are an average of six different experiments. Error bars represent \pm SD. Experimental details are provided in the text.

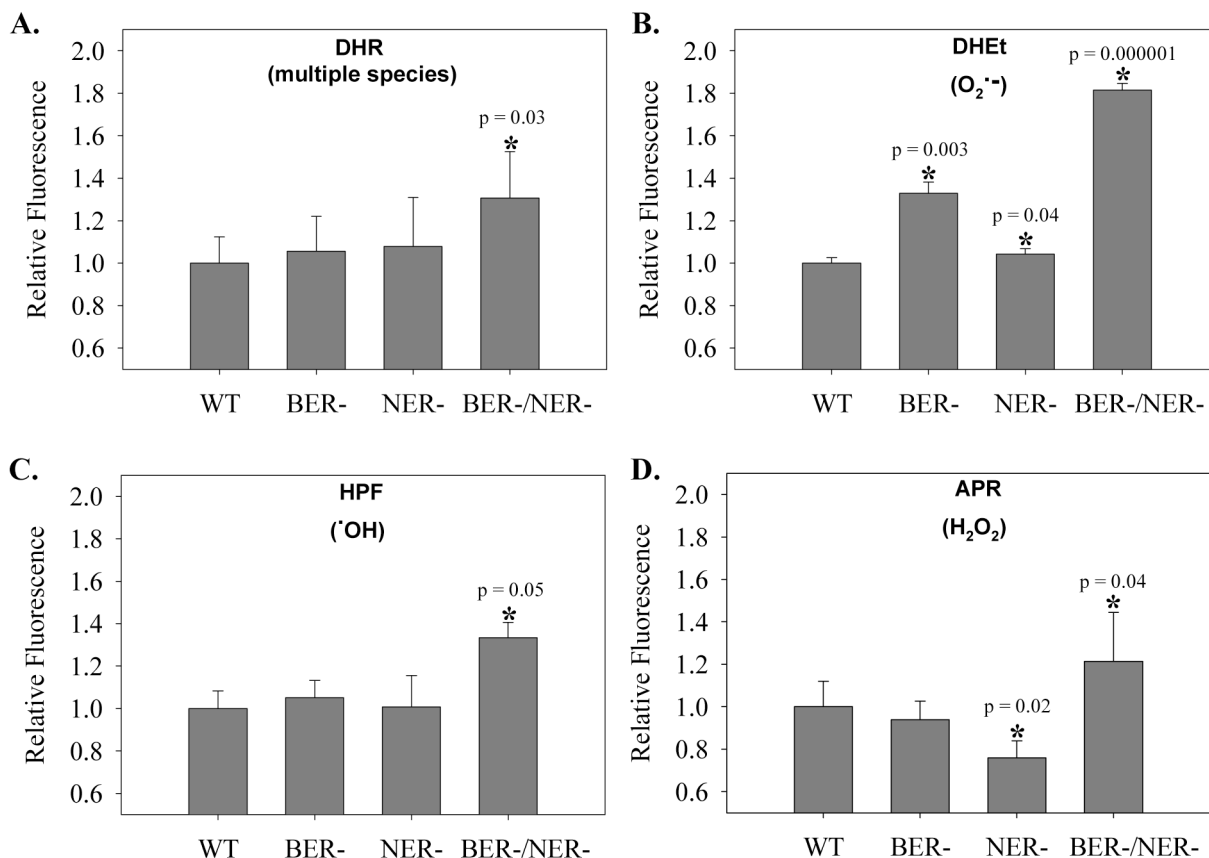


Figure 2. Endogenous levels of ROS in isogenic DNA repair-proficient and -deficient strains
 Isogenic WT, BER-, NER-, and BER-/NER- strains were incubated with the indicated fluorescent probes (A) DHR, (B) DHEt, (C) HPF, or (D) APR for 2 hours as described in Experimental Procedures. Following incubation, cells were analyzed for ROS levels by flow cytometry as described in the text. Fluorescence values were obtained from measurement of the mean peak values of the cytograms. Fluorescence values for each ROS probe are reported as the fold change relative to the WT (repair proficient) strain (set to a value of 1.0). These results are an average of three independent experiments. Error bars represent \pm SD. Asterisks above bars indicate statistical significance of a p value < 0.05 as compared to no exposure condition.

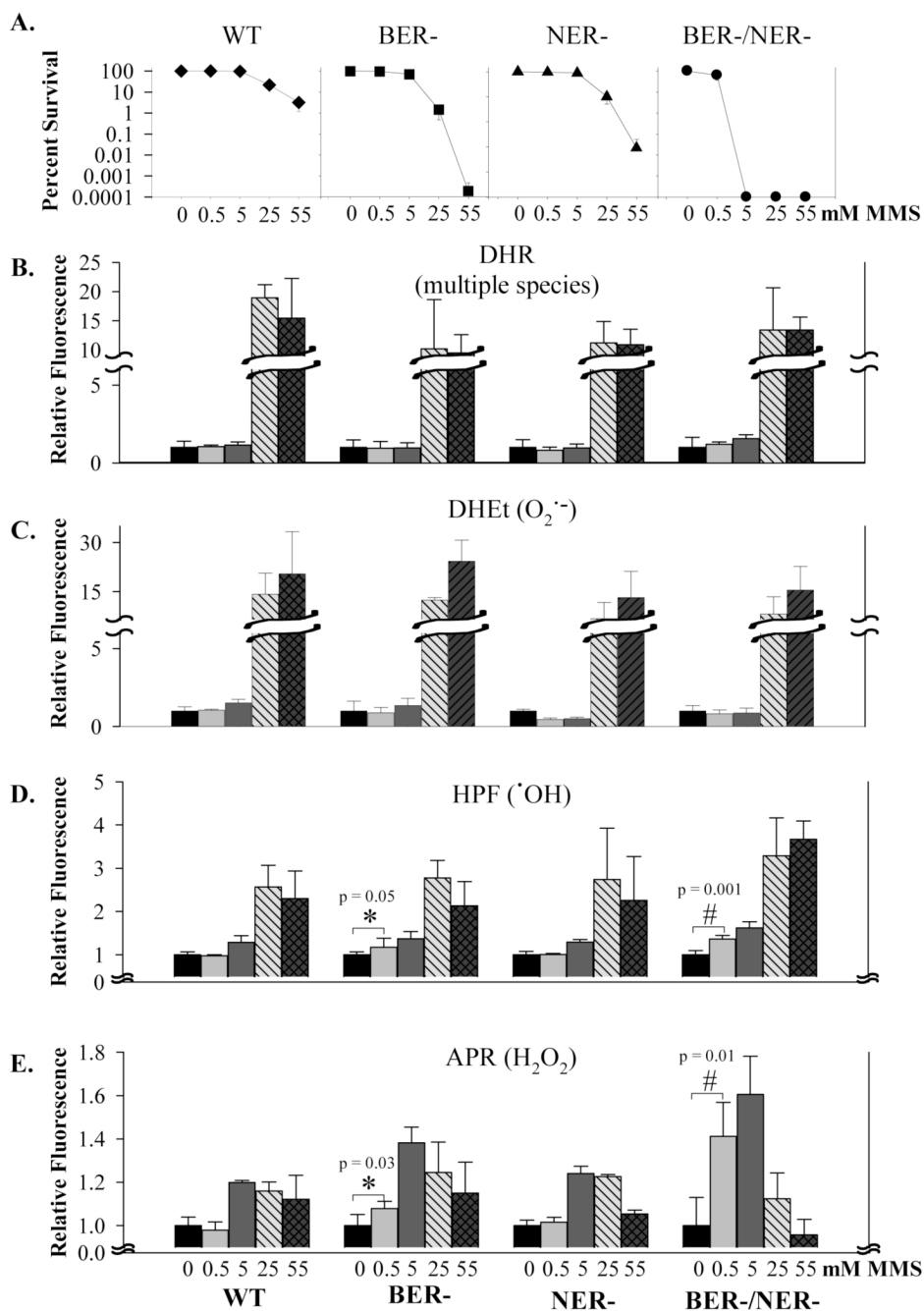


Figure 3. ROS levels in DNA repair deficient strains in response to DNA alkylation damage
A. MMS cytotoxicity of strains with different DNA repair backgrounds. WT (diamonds), BER- (squares), NER- (triangles), and BER-/NER- (circles). Cells were exposed to 0, 0.5, 5, 25, and 55 mM MMS for 30 min at 30 °C as described in the text. Results displayed are an average of six different experiments. **B – E.** Isogenic WT, BER-, NER-, and BER-/NER- strains were first exposed to MMS (0–55 mM) for 30 min and then incubated with the indicated fluorescent probes (**B**) DHR, (**C**) DHEt, (**D**) HPF, or (**E**) APR for 2 hours. Following incubation, cells were analyzed for ROS levels by flow cytometry as described in Experimental Procedures. Fluorescence values were obtained from measurement of the mean peak values of the cytograms. Fluorescence values for each ROS probe are reported as fold changes relative to

the control (0 mM MMS) for each strain (set to a value of 1.0). These results are the average from three independent experiments. Error bars represent \pm SD. “*” symbols above bars indicate statistically significant (p value <0.05) differences between the levels of H₂O₂ or •OH in BER- deficient strains at 0.5 mM MMS compared to no exposure conditions and “#” symbols above bars indicate statistically significant (p value <0.05) differences between the levels of H₂O₂ or •OH in BER-/NER- deficient strains at 0.5 mM MMS compared to no exposure conditions.

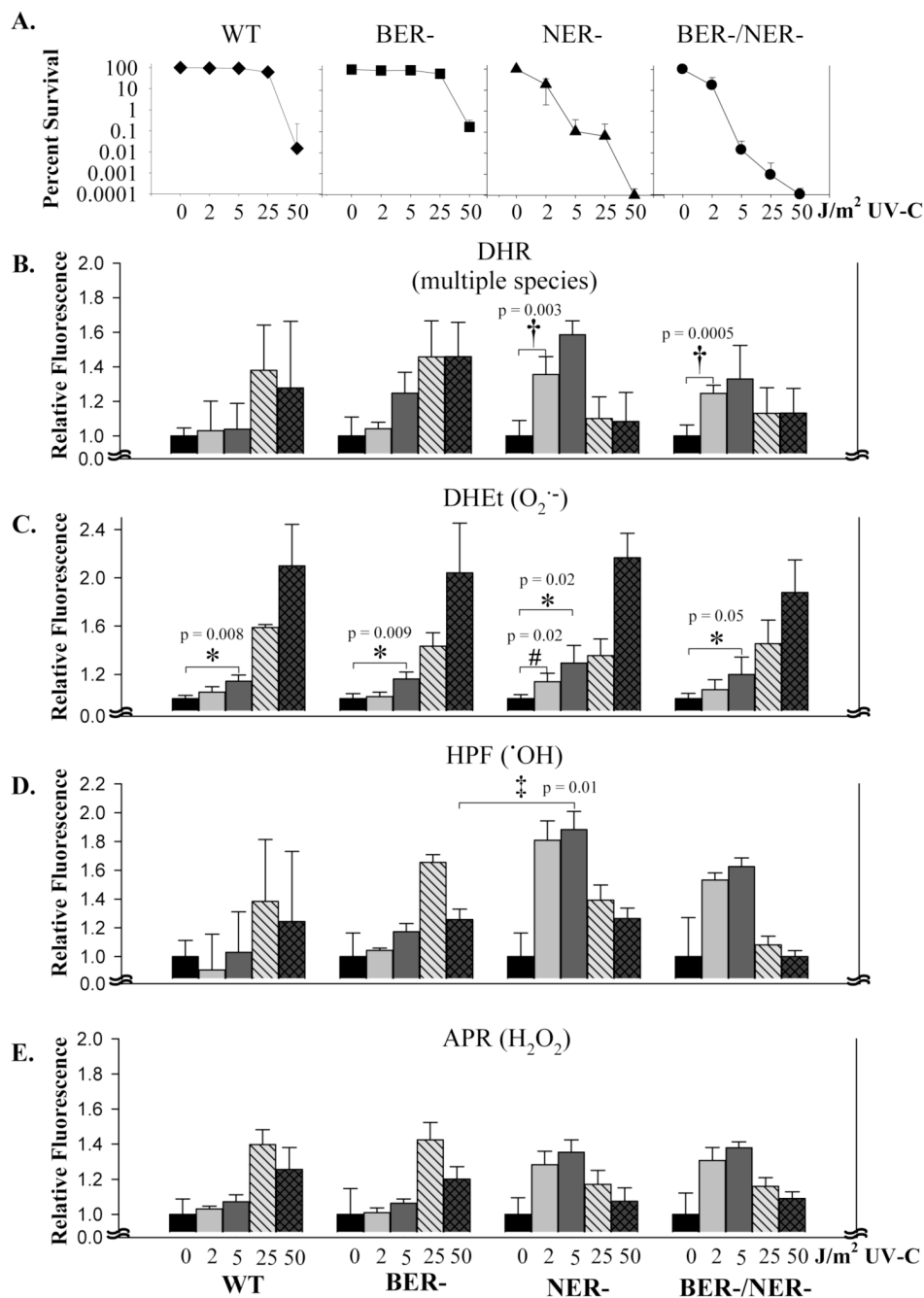


Figure 4. ROS levels in DNA repair-deficient strains in response to UV-C induced DNA damage
A. UV-C cytotoxicity of strains with different DNA repair backgrounds. WT (diamonds), BER- (squares), NER- (triangles), and BER-/NER- (circles). Cells were exposed to 0, 2, 5, 25, and 50 J/m² UV-C as described in the text. Results displayed are an average of six different experiments. **B – E.** Isogenic WT, BER-, NER-, and BER-/NER- strains were first exposed to UV-C (0–50 J/m²) and then incubated with the indicated fluorescent probes (**B**) DHR, (**C**) DHEt, (**D**) HPF, or (**E**) APR for 2 hours. Following incubation, cells were analyzed for ROS levels by flow cytometry as described in Experimental Procedures. Fluorescence values were obtained from measurement of the mean peak values of the cytograms. Fluorescence values for each ROS probe are reported as fold changes relative to the control (0 J/m² UV-C) for each

strain (set to a value of 1.0). These results are the average of three independent experiments. Error bars represent \pm SD. “*” symbols above bars indicate statistically significant (p value <0.05) differences between the levels of $O_2^{\bullet-}$ in all strains at 5 J/m² UV-C compared to no exposure conditions. “#” symbols above bars indicate statistically significant (p value <0.05) differences between the levels of $O_2^{\bullet-}$ in NER-deficient strain at 0.5 J/m² UV-C compared to no exposure conditions. “†” symbols above bars indicate statistically significant (p value <0.05) differences between the levels of ROS in NER- and BER-/NER- deficient strains at 0.5 J/m² UV-C compared to no exposure conditions. “‡” symbols above bars indicate statistically significant (p value <0.05) differences between the levels of \bullet OH at the 5 J/m² UV-C exposure in NER-deficient cells as compared to 55 J/m² UV-C exposure in BER-deficient cells.

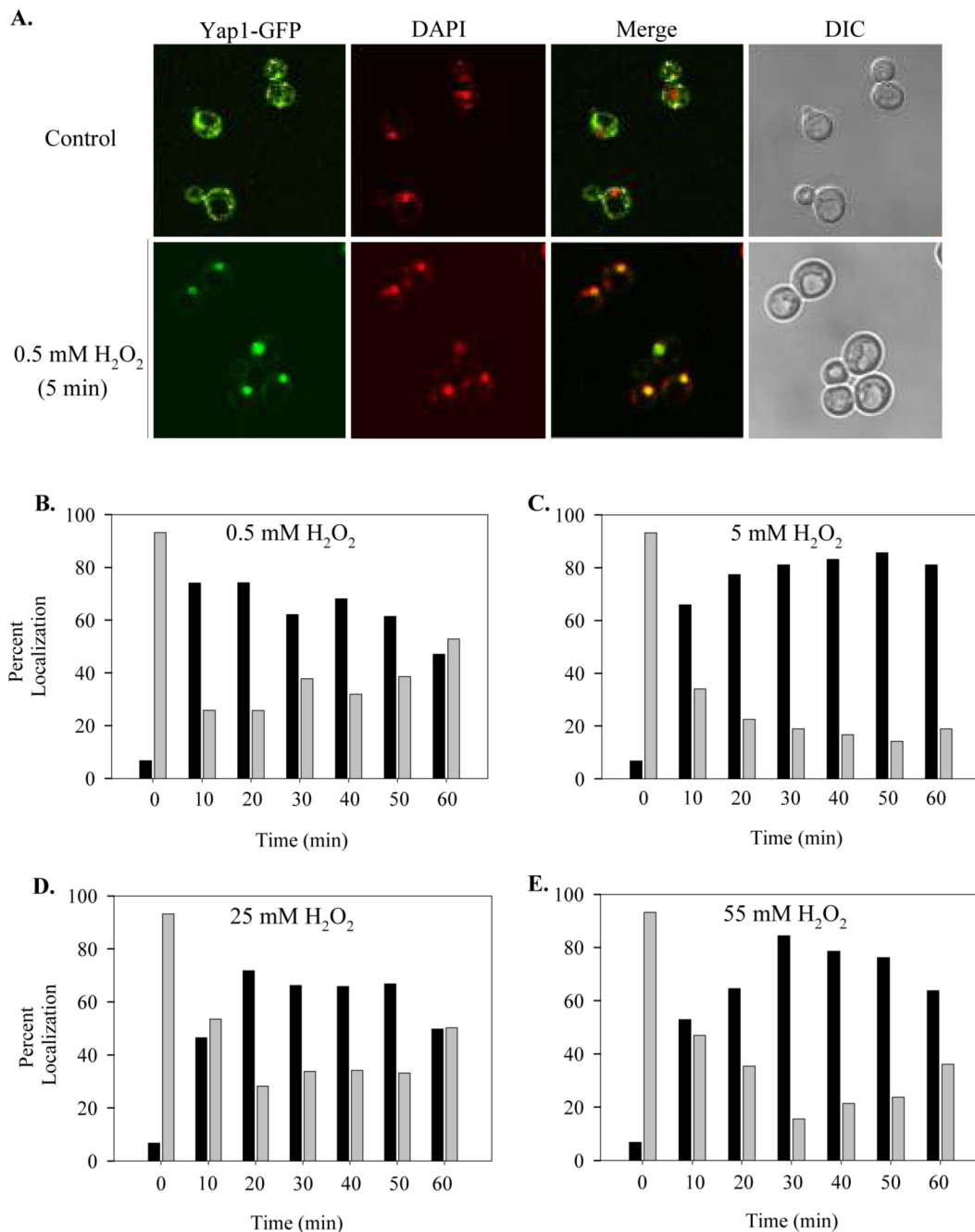


Figure 5. Yap1 localization in WT cells after exposure to H₂O₂

A. Yap1-GFP was visualized by direct fluorescence microscopy in WT cells either untreated (Control) or treated with 0.5 mM H₂O₂ for 5 min. Cells were stained with DAPI to visualize the position of the chromatin within the nuclei. The Merge image indicates the overlap (yellow) between the Yap1-GFP signal (green) and DAPI (red) staining of nuclei. Corresponding DIC images are also shown. **B–E.** Graphical representation of fluorescence microscopy analysis assessing Yap1-GFP localization. Cells were exposed to **(B)** 0.5 mM, **(C)** 5 mM, **(D)** 25 mM, or **(E)** 55 mM H₂O₂ and fluorescence images were obtained. At least 100 cells per time point from two independent experiments were counted and evaluated in 10 min interval groups. Percentages of cells scored as showing no nuclear localization (gray bars) or nuclear

localization alone or nuclear plus cytoplasmic localization for Yap1 (black bars) for every 10 minute interval group for the duration of the experiment (60 min) are indicated.

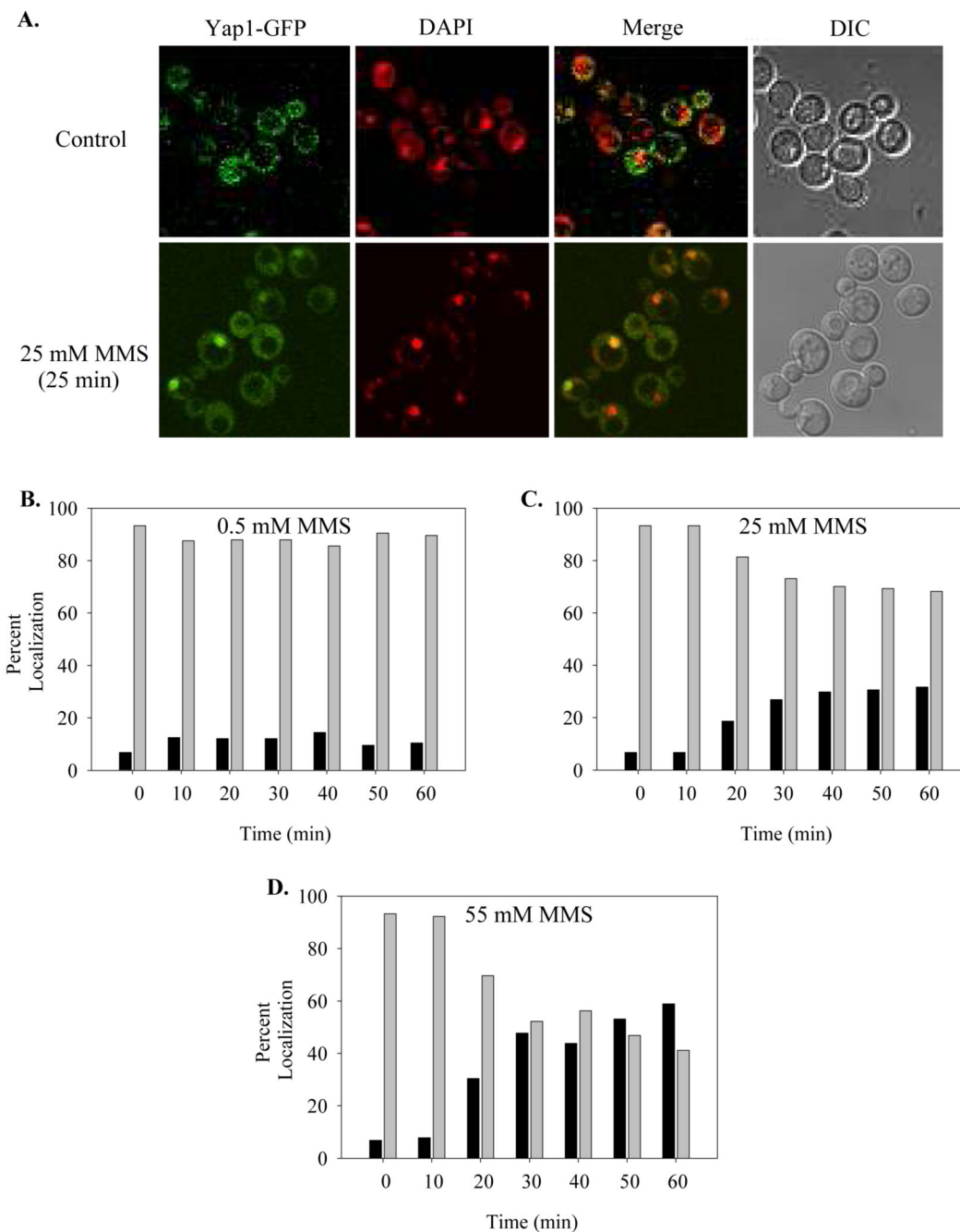


Figure 6. Yap1 localization in WT cells after exposure to MMS

A. Yap1-GFP was visualized by direct fluorescence microscopy in WT cells either untreated (Control) or treated with 25 mM MMS for 25 min. Cells were stained with DAPI to visualize the position of the chromatin within the nuclei. The Merge image indicates the overlap (yellow) between the Yap1-GFP signal (green) and DAPI (red) staining of nuclei. Corresponding DIC images are also shown. **B–D.** Graphical representation of fluorescence microscopy analysis assessing Yap1-GFP localization. Cells were exposed to **(B)** 0.5 mM, **(C)** 25 mM, or **(D)** 55 mM MMS and fluorescence images were obtained. At least 100 cells per time point from two independent experiments were counted and presented in 10 min interval groups. Cells were scored as showing no nuclear localization (gray bars) or nuclear localization alone or nuclear

plus cytoplasmic localization for Yap1 (black bars) for every 10 min interval group for the duration of the experiment (60 min) are indicated.

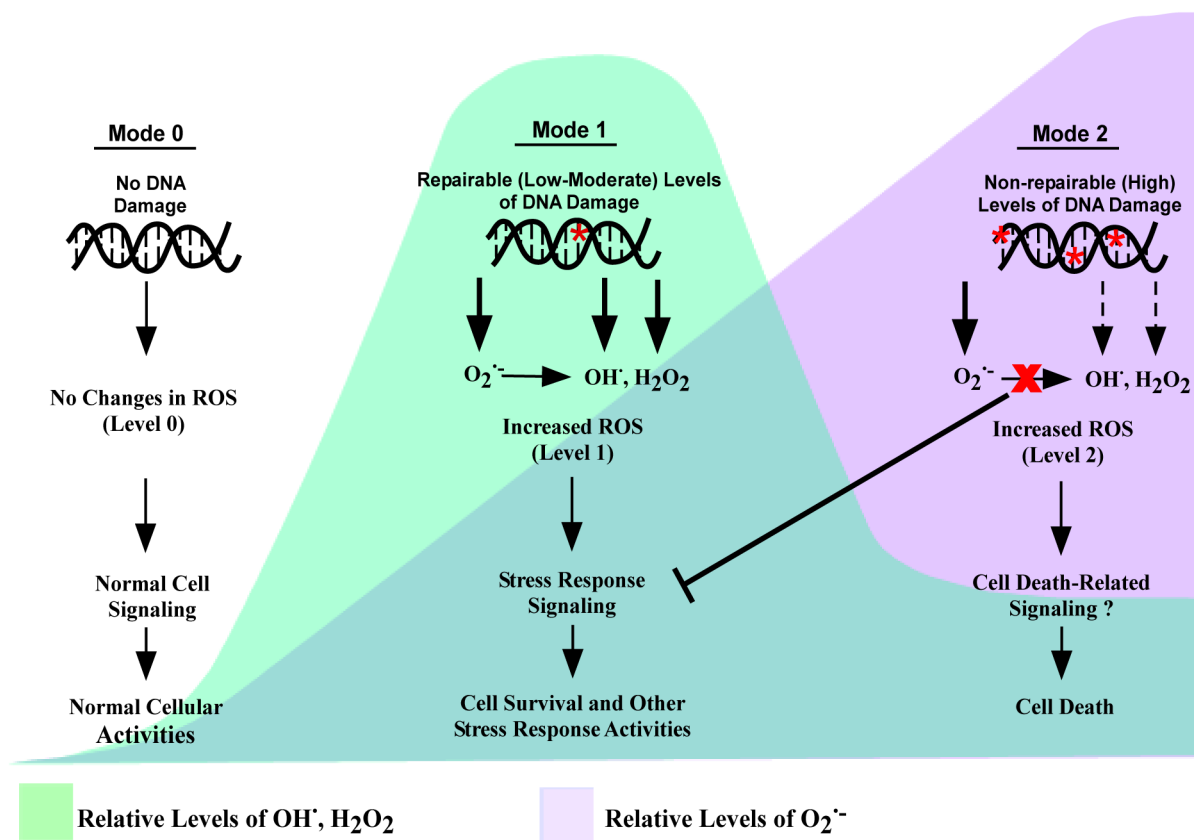


Figure 7. Model for the role of ROS in the genotoxic stress response

Under normal (no stress) growth conditions, in the absence of genomic DNA damage, the redox state of the cell is normal (Mode 0). Upon genomic DNA damage, intracellular levels of ROS increase. At low to moderate levels of DNA damage, cellular $O_2^{\bullet-}$, H_2O_2 , and OH^\bullet levels increase (Level 1). The increased levels of H_2O_2 and OH^\bullet could be caused by direct production in response to DNA damage or through conversion from $O_2^{\bullet-}$ via non-enzymatic and enzymatic pathways [44]. OH^\bullet and H_2O_2 function as signaling molecules to activate the genotoxic stress response including pathways involving SAPKs, multiphosphorelay and AP-1 like transcription factors. Each of these pathways is activated in response to changes in the redox state of the cell [45]. At higher levels of DNA damage, $O_2^{\bullet-}$ continues to increase (Level 2), while the production of H_2O_2 and OH^\bullet declines. The decrease in H_2O_2 and OH^\bullet levels could be due to a decrease in direct production or blocked conversion from $O_2^{\bullet-}$. The redox state of the cells (Mode 2) is primarily due to substantial increases in the $O_2^{\bullet-}$ levels that subsequently mediate the cell death response. The relative levels of H_2O_2 and OH^\bullet are represented by the green shaded area and the relative levels of $O_2^{\bullet-}$ are represented by the purple shaded area.